

15 **Abstract**

16 Understanding past changes in precipitation extremes could help us predict their dynamics under
17 future conditions. We present a novel approach for analyzing trends in extremes and attributing
18 them to changes in the local precipitation regime. The approach relies on the separation between
19 intensity distribution and occurrence frequency of storms. We examine the relevant case of the
20 eastern Italian Alps, where significant trends in annual maximum precipitation over the past
21 decades were observed. The model is able to reproduce observed trends at all durations between
22 15 minutes and 24 hours, and allows to quantify trends in extreme return levels. Despite the
23 significant increase in storms occurrence and typical intensity, the observed trends can be only
24 explained considering changes in the tail heaviness of the intensity distribution, that is the
25 proportion between heavy and mild events. Our results suggest these are caused by an increased
26 proportion of summer convective storms.

27 **Plain Language Summary**

28 Quantifying past trends in extreme rainfall is important because it can help us understand future
29 changes caused by global warming. Climate scientists and hydrologists use specific statistical
30 models to do so, but interpreting the results is complicated because extremes are rare and the
31 structure of the models is not linked to the local meteorology. We use a new statistical model that
32 allows to better understand the mechanisms behind the trends we detect. We find that extreme
33 rainfall in the eastern Italian Alps increased over the past decades and we associate this change to
34 an increased proportion of summer thunderstorms.

35 **1 Introduction**

36 Understanding past and future changes in extreme subdaily precipitation intensities is of
37 enormous interest because they are responsible for flash floods, urban floods, landslides and
38 debris flows, and cause numerous casualties and huge damages every year (Borga et al., 2014;
39 Cristiano et al., 2017; Paprotny et al., 2018). Physical laws translate increasing atmospheric
40 temperature into increasing water vapor holding capacity. Together with changes in the
41 atmospheric dynamics, this is expected to drive future precipitation changes (Trenberth et al.,
42 2003; Pendergrass et al., 2020; Fowler et al., 2021b). In general, larger responses are expected for
43 precipitation extremes because mean precipitation, on a global scale, is limited by energy
44 constraints (Allan and Soden, 2008; Pendergrass & Hartmann, 2014). However, detecting
45 changes in extreme precipitation is highly affected by the stochastic uncertainty characterizing
46 the sampling of extremes. This uncertainty may mask the influence of climate forcing on the
47 processes which locally control the extremes (Fatichi et al., 2016; Marra et al., 2019).

48 Statistically significant changes in the frequency of extreme precipitation in the past
49 decades were reported, often with stronger trends in subdaily extremes, as opposed to daily
50 (Guerreiro et al., 2018; Markonis et al., 2019; Papalexiou & Montanari, 2019). In some cases,
51 opposing trends between short and long durations emerged, with complex implications for flood
52 risk (Zheng et al., 2015). Available observations show different temporal trends for precipitation
53 intensities associated to different exceedance probabilities (Schär et al., 2016; Pendergrass,
54 2018). In general, increasing trends are reported for rarer events (Myhre et al., 2019), but the
55 specific differences depend on duration, season, and local conditions, such as the dominating
56 meteorological features contributing extremes (Blanchet et al., 2021; Moustakis et al., 2021).

57 Extreme return levels characterized by different exceedance probabilities are thus changing at
58 different rates (Myhre et al., 2019; Marra et al., 2021).

59 Nonstationary extreme value models could aid the detection and quantification of trends
60 in extreme precipitation of different exceedance probability (e.g., Min et al. 2009). However, the
61 information these models can provide is impacted by stochastic uncertainties (Serinaldi and
62 Kilsby, 2015; Fatichi et al., 2016), and their flexibility is limited by the assumptions concerning
63 high order statistical moments. In fact, due to intrinsic limitations in parameter estimation
64 accuracy, the shape (and sometime also the scale) parameter of the extreme value distribution is
65 assumed to be constant (Prodocimi and Kjeldsen, 2021). Additionally, due to the structure of
66 these statistical models, a link between the properties of the underlying process, such as
67 precipitation occurrence frequency and intensity distribution, and extremes is difficult to
68 establish (e.g. Marra et al., 2019). As such, the possibility to attribute the observed changes to
69 specific physical and meteorological processes is hampered.

70 This background suggests that there is a need to move beyond traditional trend detection
71 techniques applied to extremes only and develop novel methodologies. These methods should be
72 able to detect general changes in extreme precipitation at multiple durations, quantify changes at
73 different exceedance probabilities, and attribute these to changes in the underlying physical
74 processes.

75 A recent methodology for extreme precipitation frequency analysis, termed Metastatistical
76 Extreme Value (MEV) (Marani and Ignaccolo, 2015), provides grounds for addressing these
77 issues. The approach relies on the concept of *ordinary events*, that is all the independent
78 realizations of a process of interest, and proved highly effective in reducing stochasting
79 uncertainties (Zorretto et al., 2016; Marra et al., 2018). As opposed to traditional methods, MEV
80 assumes the distribution describing the ordinary events is known, and derives an extreme value
81 distribution by explicitly considering (i) occurrence frequency of the ordinary events, and (ii)
82 inter-annual variability of their intensity distribution and of their occurrence frequency. Multiple
83 types of ordinary events and their temporal changes can be directly considered in the formalism
84 (Marra et al., 2019). The parameters describing the ordinary events intensity distribution and
85 their yearly number are thus treated separately, and are estimated on a yearly basis, providing
86 great potential for trend detection and attribution studies (Miniussi and Marani, 2020; Marra et
87 al., 2021).

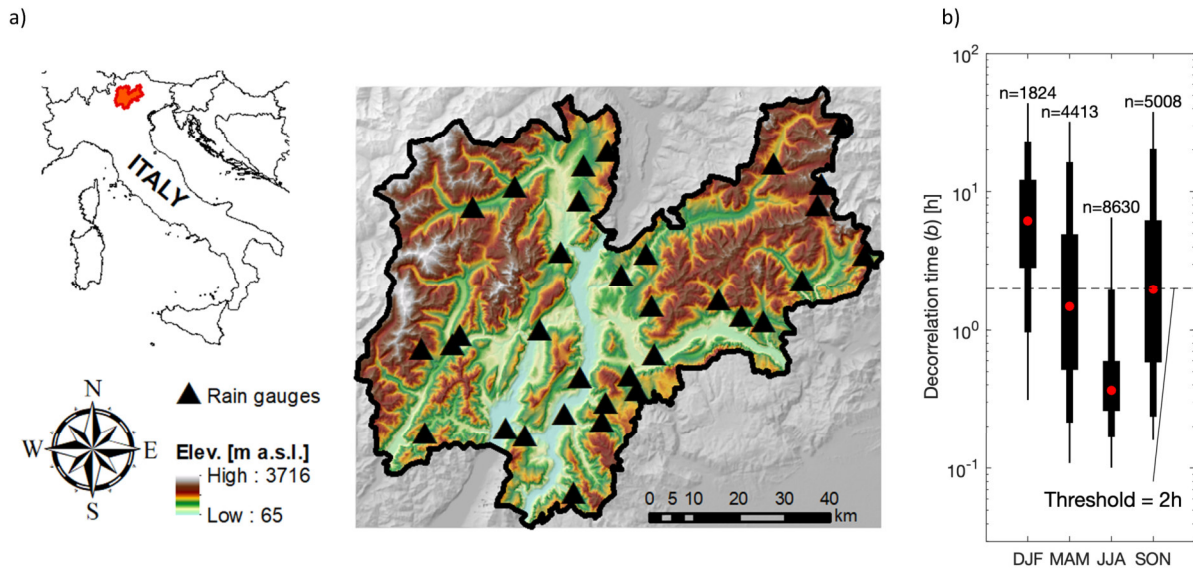
88 Here, we combine a novel approach for ordinary-events-based precipitation frequency
89 analyses across durations (Marra et al., 2020) with a regional trend detection technique to: (a)
90 detect and quantify trends in sub-daily annual maxima and extreme return levels by
91 independently considering the changes in statistical properties and occurrence frequency of
92 storms, and (b) attribute the observed trends in extremes to specific changes in the local
93 precipitation regime. We examine the relevant case of the eastern Italian Alps, where consistent
94 significant changes in annual maximum precipitation intensities at subdaily and daily duration
95 were reported (Libertino et al., 2019).

96 **2 Data and methodology**

97 **2.1 Study area and data**

98 We focus on Trentino, a 6000 km²-wide mountainous area in the Eastern Italian Alps
99 (**Figure 1a**) which experienced significant increases in extreme short-duration rain intensities

100 over the last decades (Libertino et al., 2019). Mean annual precipitation varies from ~ 1300 mm
 101 yr^{-1} in the south-eastern portion of the area to lower amounts (~ 900 mm yr^{-1}) typical of the “inner
 102 alpine province” in the north (Borga et al., 2005). A dense network of more than one hundred
 103 rain gauges is present. From these, 33 stations (density $\sim 1/190$ km $^{-2}$) with at least 25 complete
 104 years ($<10\%$ missing data) of 5-minute resolution data in the period 1986-2019 are selected
 105 (**Figure 1a**; see Table S1 in the Supporting Information).



106

107 **Figure 1. a)** Location and orographic structure of the study area and location of the rain gauges
 108 used in this study; b) Decorrelation time of the highest 25% ordinary events organized by season.
 109 The red dots indicate the median values; bars indicate percentiles: 25-75th, 5-95th, 1-99th. The
 110 number of storms occurred across the stations in each season is reported.

111 2.2 Methodology

112 The MEV approach expresses the cumulative distribution $\zeta(x)$ of extreme return levels x
 113 as a function of the yearly cumulative distributions of the ordinary events $F(\cdot)$ and their yearly
 114 number of occurrences (Marani and Ignaccolo, 2015; Zorzetto et al., 2016):

115
$$\zeta(x) = \frac{1}{M} \sum_{j=1}^M F(x, \theta_j)^{n_j}$$
, where θ_j are the parameters describing the yearly distribution
 116 $F(\cdot)$ in the j -th year, n_j the corresponding number of ordinary events, and M is the number of
 117 years in the record. Indirectly, this formalism allows us to quantify return levels from individual
 118 years using the $\zeta_j(x) = F(x; \theta_j)^{n_j}$, thus allowing to directly quantify trends in return levels
 119 themselves.

120 Previous studies show that subdaily precipitation intensities require three- (or more)
 121 parameters distributions to be fully described (Papalexiou et al., 2018). However, their right tails
 122 can be well approximated using a two-parameter distribution which, in many cases, is found to
 123 be a Weibull distribution (e.g., Zorzetto et al. 2016; Marra et al., 2020). This means that a portion
 124 of their distribution including the extremes can be approximated as $F(x, \lambda, \kappa) = 1 - e^{-\left(\frac{x}{\lambda}\right)^\kappa}$,
 125 where λ is a scale parameter and κ is a shape parameter which determines the tail heaviness:

126 higher shape parameters are associated to lighter tails, and vice versa (see Figure S1). In
 127 particular, the tail is sub-exponential for $\kappa > 1$, exponential for $\kappa=1$, and heavier than exponential
 128 for $\kappa < 1$. The number of yearly events modulates the tail of the extreme value distribution $\zeta(x)$.

129 The here presented analysis is based on the storm-based definition of ordinary events
 130 proposed by Marra et al. (2020). For each station, “storms” are defined as wet periods separated
 131 by dry hiatuses of predefined length. We define as wet all the 5 min time intervals reporting at
 132 least 0.1 mm of precipitation, and separate storms using 24 hr dry hiatuses. A minimum duration
 133 of 30 min for a single storm is set to avoid individual tips to be considered as storms. Ordinary
 134 events are then defined as the maximum intensities observed over the duration of interest in each
 135 storm (details in Marra et al., 2020). Durations between 15 min to 24 hr are explored. For each
 136 station and duration, we derive temporal series of ordinary events and, for each year, we estimate
 137 parameters of the Weibull distribution by left censoring the portion of data which is deemed not
 138 representative of the tail. We use the least-squares method in Weibull-transformed coordinates
 139 (Marani and Ignaccolo, 2015). The choice of the left-censoring threshold follows the test
 140 described in Marra et al. (2020): the distribution parameters are estimated for different thresholds
 141 by explicitly censoring the observed annual maxima; the maxima are then compared to the
 142 sampling confidence interval from the estimated distribution to assess whether they could be
 143 likely samples. Following the method suggested in Marra et al. (2019), we select the 75th
 144 percentile of the ordinary events for the left-censoring. This is in line with previous findings in
 145 different areas (Marra et al., 2019; Marra et al., 2020). It should be recalled that the selection
 146 method implies a low sensitivity of the results to this threshold. After left-censoring, an average
 147 of ~14 ordinary events per year are used for parameter estimation. Yearly return levels are
 148 obtained by inverting the equation for $\zeta_j(x)$ (Zorzetto et al., 2016). In this way, we obtain, for
 149 each station, yearly series of scale parameter, shape parameter, number of ordinary events, and
 150 return levels. Annual maxima (AM) series are also extracted.

151 We investigate the presence of monotonic trends in these quantities using the Regional
 152 Mann-Kendall test at the 0.05 significance level (Mann, 1945; Kendall, 1975; Helsel & Frans,
 153 2006), and we quantify the average rate of change using the nonparametric Sen’s slope estimator
 154 (Sen, 1968). Serial correlation in the series was tested and found negligible. In case trends within
 155 the region are heterogeneous, the slope and significance estimated by the Regional Mann-
 156 Kendall test could be misleading (Gilbert, 1987). We verify the homogeneity among the trends at
 157 the different sites in the area by applying the Van Belle and Hughes test (1984). We find that
 158 homogeneity is verified for all the investigated variables. As spatial correlation among nearby
 159 stations could decrease the power of regional test, we include the correction proposed by Hirsch
 160 and Slack (1984).

161 The null hypothesis of the Mann-Kendall test is true (i.e., no trend) when about half of
 162 the pair comparisons between ordered each data points is concordant and half discordant.
 163 Considering that 2 yr return levels correspond to the theoretical median of the AM, we consider
 164 the estimated trend on the 2 yr return levels as our model quantification of the trend in the AM.

165 The ability of our statistical model to reproduce observed trends in AM is verified by
 166 accounting for stochastic uncertainty in a Monte Carlo framework. For each station i , year j and
 167 duration d , n_{ijd} Weibull-distributed ordinary events are generated according to the distribution
 168 parameters λ_{ijd} and κ_{ijd} , and the AM are extracted. The procedure is iterated 1000 times (which
 169 was found to provide coherent estimates of the 90% confidence interval), to obtain 1000
 170 synthetic regional sets of AM series for each duration. The Regional Mann-Kendall test is then

171 performed on these sets to obtain 1000 slopes estimates for each duration, which provide a
172 quantification of the stochastic uncertainty in the trends of the modelled AM.

173 A sensitivity analysis is performed for evaluating the relative impact of trends in the
174 model parameters on the emerging trend in the modelled AM. For each station and duration, the
175 trends on modelled AM are computed using different combinations in which inter-annual
176 variability in the parameters is either considered or ignored. In the latter case, the median
177 parameter is used. We thus obtain the following cases: one case with 3 time-varying parameters
178 (real case), 3 combinations of 2 varying and 1 constant parameter, 3 combinations of 1 varying
179 and 2 constant parameters, and one case of 3 constant parameters (no-change). Then the
180 Regional Mann-Kendall test is applied to the resulting series.

181 Changes in the seasonal proportions between convective-like and other event types in
182 different seasons are explored to investigate the seasonal and physical mechanisms underlying
183 the observed trends. Events exceeding the left-censoring threshold at any of the durations are
184 organized by seasons. The temporal decorrelation of the rain intensity timeseries is used as a
185 proxy for broadly distinguishing between convective-like and other types of storms. The
186 decorrelation time (**Figure 1b**) is taken equal to the scale parameter of the exponential fitting of
187 the temporal autocorrelation. This is thus the time lag at which the temporal autocorrelation
188 drops to e^{-1} . The average (across stations) number of storms belonging to the two groups is
189 calculated for each season, and the significance and slope of their trend is estimated using the
190 Mann-Kendall test ($p=0.05$) and the Sen's slope estimator. This shows if temporal changes in the
191 proportion of different event types in the seasons emerged. A 2 hr threshold is found to optimally
192 describe (that is, optimize the statistical significance) the temporal changes in our data and is
193 therefore used as a proxy for distinguishing between convective-like (decorrelation time ≤ 2 hr)
194 and other event types (> 2 hr). Qualitatively analogous outcomes are obtained with thresholds
195 between 1 and 3 hr.

196 **3 Results and discussion**

197 3.1 Regional trends on multi-duration extremes

198 Slopes for the regional trends for the nine investigated durations are reported in **Figure**
199 **2a**. Hereinafter, slopes are normalized over the median value of each variable and expressed as
200 percent change per year. As expected (Libertino et al., 2019), observed AM show positive trends
201 at all durations. Statistically significant trends are observed for durations below 6 hours and
202 stronger increases for hourly and sub-hourly durations. The slopes estimated using the MEV
203 model ("modelled AM" in **Figure 2**) lie within the 90% confidence interval due to stochastic
204 uncertainty (grey area), indicating that they are likely samples from our model. This means that
205 the model well reproduces the trends in the observed AM.

206 The annual number of storms, uniquely defined for all durations (Marra et al., 2020),
207 shows a significant increase ($4\% \text{ yr}^{-1}$) (**Figure 2b**). Trends in the scale parameter of the intensity
208 distributions are always positive, indicating a general increase in the intensity of the largest 25%
209 of the ordinary events, with larger and significant increases (up to $8\text{-}9\% \text{ yr}^{-1}$) for multi-hour
210 durations (**Figure 2b**). The shape parameter shows negative trends for sub-hourly durations and
211 positive trends for longer durations (**Figure 2b**), indicating that the proportion between heavy
212 and mild events changed in different ways for short and long durations: increased tail heaviness
213 is reported for sub-hourly durations and decreased tail heaviness for multi-hour durations (see

214 Figure S1 for a visual interpretation of the effect of the shape parameter on tail-heaviness). At
215 short durations the changes in the two parameters have a synergistic impact on extremes.
216 Although the trend in individual parameters is not significant, observed and modelled AM
217 experience stronger and significant changes. In contrast, at longer durations the changes in the
218 parameters have opposing impact on extremes, and AM exhibit weaker increases, despite the
219 significant increase of both scale parameter and yearly number of storms. In particular, where
220 tail-heaviness has its strongest significant decrease (increase in the shape parameter), trends in
221 extremes are at a minimum and are not significant.

222 These findings indicate that in the examined period (1986-2019) and area, AM exhibit
223 significant changes, in particular for short-duration intensities, in agreement with previous
224 studies (Libertino et al., 2019). Overall, our statistical model reproduces these trends accurately,
225 and allows us to investigate the underlying statistical mechanisms. Changes in AM seem to be
226 mostly influenced by changes in the tail-heaviness of the ordinary events, although trends in the
227 shape parameter itself are not statistically significant.

228 3.2 Sensitivity of the changes in annual maxima to changes in intensity, occurrence
229 frequency and tail heaviness of the ordinary events

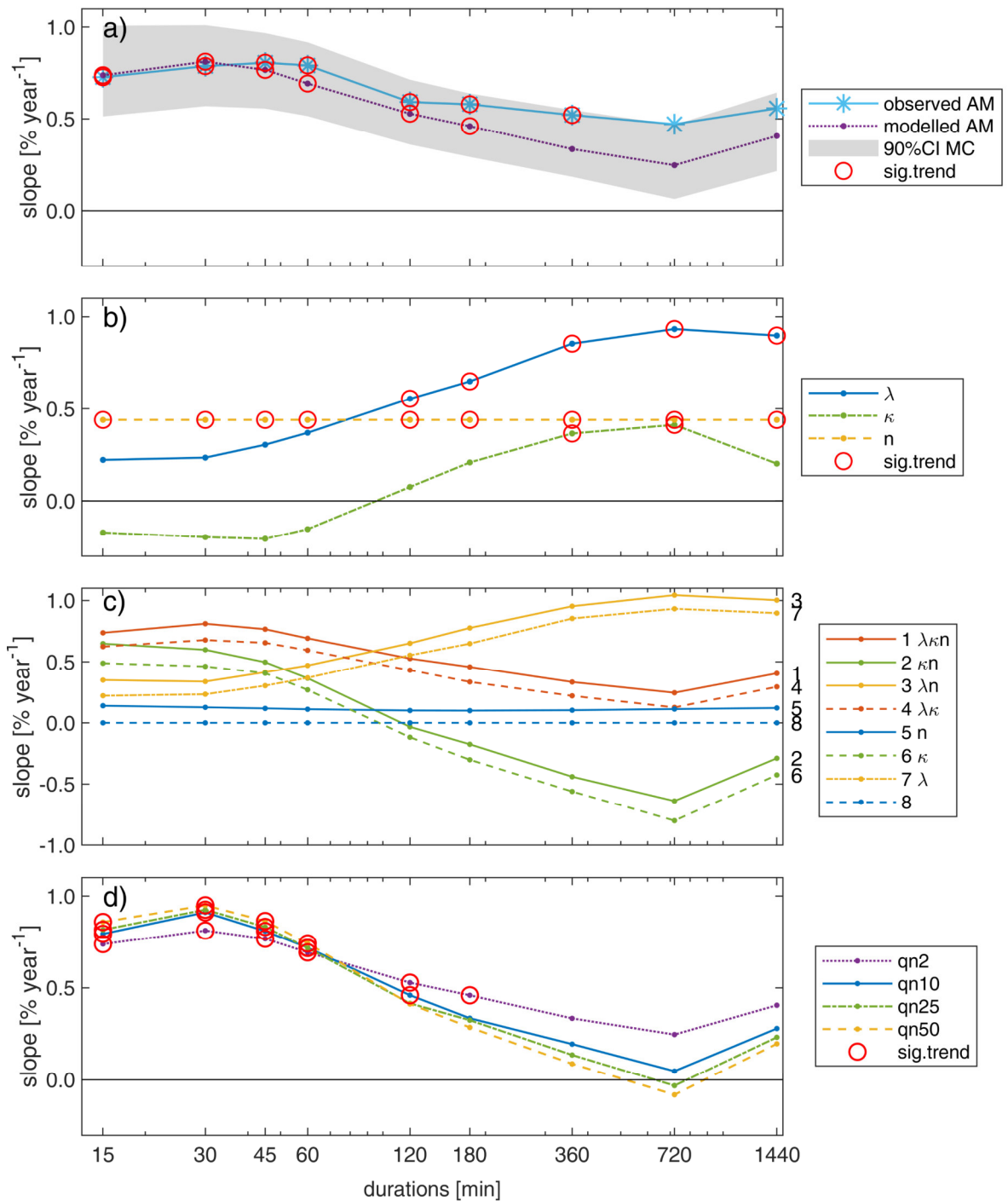
230 We investigate the sensitivity of the trends in AM to trends in the individual model
231 parameters (**Figure 2c**). The ‘real’ case in which all parameters change with time reproduces the
232 trends in the modelled AM (line 1 in **Figure 2c**). The other lines are a combination of varying
233 and constant (median) parameters. Notably, the significant increase ($+4\% \text{ yr}^{-1}$) in the number of
234 yearly storms only has a marginal impact on the overall trends in extremes (same-color pairs of
235 lines). Synergistic and opposing impacts of the other parameters are mostly evident by
236 comparing the constant scale-parameter case (line 2) with the constant tail-heaviness case (line
237 3). When no changes in tail-heaviness are considered, AM show increasing trends whose
238 magnitude can even increase with duration, instead of decreasing (lines 3, 7). This sensitivity
239 analysis shows that little changes in the tail-heaviness (shape parameter) turn into large changes
240 in extreme intensities, suggesting this is an important parameter explaining the observed AM
241 trends in the region. Crucially, without considering changes in tail heaviness it is not possible to
242 explain the large observed increase in short-duration AM, as well as the different response of
243 short and long duration extremes. This has profound implications for change-permitting extreme
244 value models in which tail heaviness is often assumed to remain constant.

245 3.3 Regional trends of extreme return levels

246 Our statistical model allows to directly quantify changes on specific rare return levels. In
247 general, slopes are always significantly positive for sub-hourly durations and decrease with
248 increasing duration until they lose significance for durations above 2-3 hr (**Figure 2d**). For
249 higher return levels, this behavior is enhanced: higher positive slopes are estimated for subhourly
250 durations and lower slopes for multi-hour durations, even approaching no-trend or negative-trend
251 behaviours for 25 and 50 yr return levels and 12-24 hr duration. There is a duration interval
252 between 1 and 2 hr where the trends don’t depend on return period, closely following the change
253 in regime in which the trend in the shape parameter crosses zero, that is no change in tail
254 heaviness.

255 The here adopted statistical framework gives the opportunity to quantify and evaluate the
256 statistical significance of trends in rare return levels of interest for hydrological design and risk

257 management. It could be argued that estimating rare quantile on a yearly basis should lead to
 258 unberable uncertainties. We showed here that the statistical significance of trends in yearly-
 259 modelled return levels as high as the 50 yr events is comparable to the statistical significance of
 260 trends in AM, suggesting a similar signal to noise ratio. Trends on extreme return levels
 261 estimated on yearly basis from our model are thus characterized by stochastic uncertainties
 262 comparable to the ones of AM.

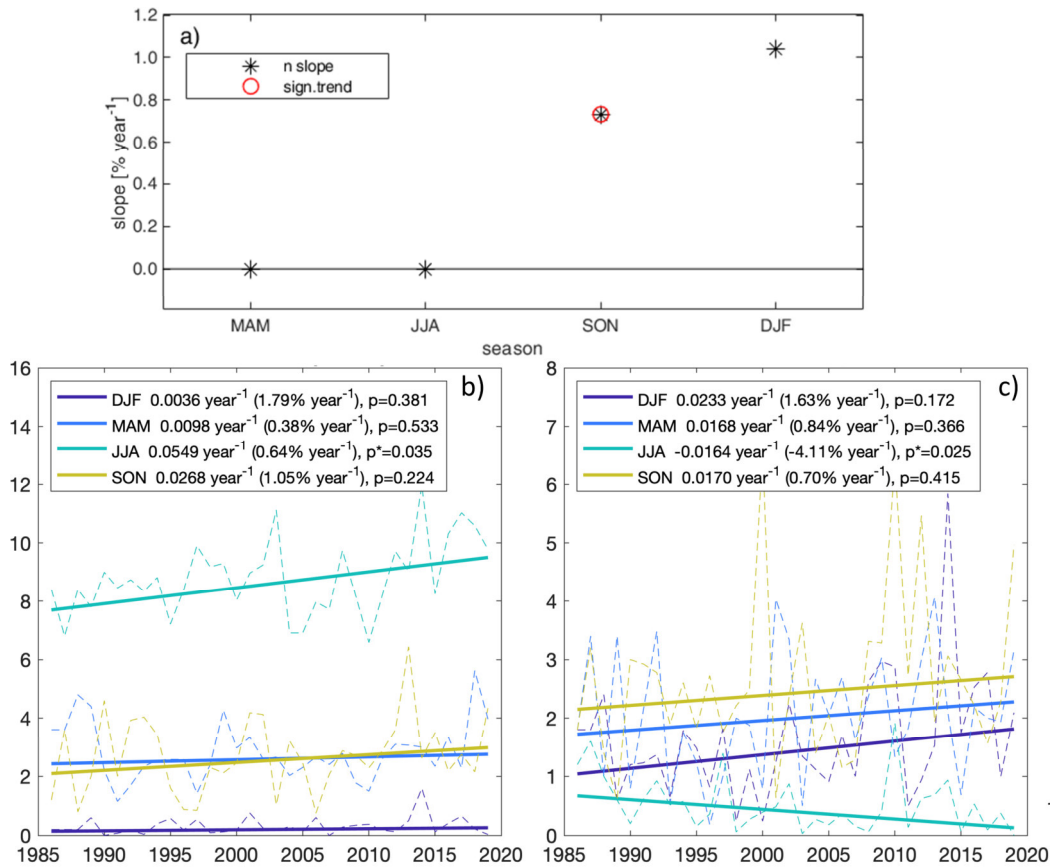


264 **Figure 2. a)** Slopes of the regional trends at different durations for observed and modelled AM;
265 significant trends ($p=0.05$) are marked; stochastic uncertainty associated with the modelled AM
266 (90% C.I. of the MonteCarlo simulation) is also reported. **b)** Slopes of the regional trends for the
267 model parameters: scale parameter (λ), shape parameter (κ), and yearly number of storms (n);
268 significant trends ($p=0.05$) are marked. **c)** Sensitivity of the modelled trends to combinations of
269 changes and no-changes in the model parameters; series labels report the parameters which are
270 allowed to change. **d)** Slopes of the regional trends for some estimated return levels (2, 10, 25,
271 50 yr); significant trends ($p=0.05$) are marked; note that the 2 yr return levels correspond to the
272 modelled AM.

273 3.4 Changes in the proportion of convective-like events

274 The parametrization of our model allows us to formulate hypotheses about the physical
275 processes underlying the detected changes. In particular, the observed changes could be
276 explained by an increased number of intense convective events, which would mainly contribute
277 to the short duration annual maxima. We analyze possible changes in the number of storms
278 occurring in different seasons, and in the seasonal number of convective-like and other types of
279 storms (**Figure 3**). The significant positive trend in the yearly number of storms reported above
280 is fully explained by a significant increase in the number of storms in autumn (SON, **Figure 3a**)
281 and a non-significant increase in winter (DJF). However, examining changes in the types
282 composition shows no distinct increase in convective-like storms during these seasons (**Figure**
283 **3b, c**).

284 Conversely, although no trend emerges in the number of storms in summer (JJA), the
285 number of summer convective-like storms in this season increased significantly, while the
286 number of other storms decreased significantly (**Figure 3b, c**). This implies a significant increase
287 in the proportion of summer convective-like events. Since convective-like storms are generally
288 associated with heavy intensities at short durations, this change in composition could explain the
289 observed increase in tail heaviness at short durations, and thus the observed trends on short-
290 duration AM. This is confirmed when the parameters of the ordinary events distribution are
291 examined considering spring-summer (MAMJJA) and autumn-winter (SONDJF) separately
292 (**Figure S2**). These results suggest that the significant positive trends found for short-duration
293 extremes are mostly related to changes in summer storms, and that these can be related to
294 changes in the intensity distributions (increasing tail-heaviness) induced by an increasing
295 proportion of heavy convective-like storms in the summer.



296

297 **Figure 3. a)** Slope of the regional trends for the number of seasonal storms; significant trends
 298 ($p=0.05$) are marked. **b)** Average (across stations) seasonal number of convective-like
 299 (decorrelation time < 2 hr) and **c)** other (decorrelation time > 2 hr) storms; the Sen's slope and
 300 the p-value of the Mann-Kendall test are reported; asterix (*) indicates significant trends
 301 ($p=0.05$).

302 5 Conclusions

303 We examine changes in extreme sub-daily precipitation intensities for the relevant case of
 304 the eastern Italian Alps, where consistent significant changes in annual maximum (AM)
 305 intensities were reported (Libertino et al., 2019). Specifically, we aim at detecting and
 306 quantifying trends in sub-daily AM and extreme return levels, and linking the observed trends in
 307 extremes to specific changes in the local precipitation regime. To do so, we adopt a novel unified
 308 framework for extreme value analyses based on ordinary events, and we quantify trends by
 309 means of the regional Mann-Kendall test. With respect to traditional change-permitting extreme
 310 value models, the here presented method provides a statistical tool for better quantifying changes
 311 in extremes in spite of the large stochastic uncertainties, and for better understanding the
 312 observed changes by separately considering multi-duration storm intensity distributions and
 313 storm occurrence frequency. The approach can be expanded to directly consider different types of
 314 storm events (Marra et al., 2019).

315 Results confirm the presence of significant positive trends in the AM. Trends in the 2 yr
316 return levels estimated yearly using our model are consistent with the observed trends in AM.
317 These trends are more marked for 15 min to 1 hr durations and less marked for 3 hr to 24 hr
318 durations. The model parametrization allows to conclude that these trends are likely due to a
319 combination of (i) increasing number of storm events per year and increasing intensity of the
320 storms, and (ii) changes in the tail properties of the storms. In particular, an increasing, albeit
321 not-significant, trend in tail heaviness at short durations seems to mostly explain the changes in
322 AM and return levels. A significant increase in the proportion of convective-like storms is
323 detected during the summer (JJA). This could explain the observed trends in AM and return
324 levels emerged at the short durations in the previous analyses, and is in agreement with results
325 reported by Fowler et al. (2021a), who highlight that the stronger increases in short-duration
326 extremes are related to feedbacks in convective clouds dynamics at the local scale.

327 The here-reported trends are derived from a relatively short data series and should be
328 considered as representative of the examined period only (1985-2019). Due to decadal climate
329 variability, they should not be considered as representative of climate change in general, nor
330 extrapolated to predict future conditions (Iliopoulou and Koutsoyiannis, 2020). Nevertheless,
331 considering the increasing attempts of the scientific community to quantify changes in
332 hydrometeorological extremes with rare yearly exceedance probability, our model could provide
333 insights for better describing local climatologies under change, and for extending our
334 understanding of changes in the underlying physical processes. This information can be valuable
335 for improving our ability to create and use process-based change-permitting statistical models for
336 hydrometeorological extremes.

337 **Data Availability Statement**

338 Precipitation data was provided by the Provincia Autonoma di Trento and can be
339 retrieved from <https://www.meteotrentino.it> (Accessed: October 2020). The codes used for the
340 MEV analyses are available at <https://doi.org/10.5281/zenodo.3971558>. The executable for the
341 Regional Mann-Kendall test (Helsel & Frans, 2006) was downloaded from
342 <https://pubs.usgs.gov/sir/2005/5275/downloads>.

343 **Acknowledgements**

344 The authors declare no conflict of interests. This study was funded by Provincia
345 Autonoma di Trento through Accordo di Programma GPR. FM thanks the Institute of
346 Atmospheric Sciences and Climate (ISAC), National Research Council of Italy for the support.

347 **References**

- 348 Alexander, L. V., N. Tapper, X. Zhang, H. J. Fowler, C. Tebaldi, and A. Lynch (2009), Climate
349 extremes: Progress and future directions, *Int. J. Climatol.*, 29, 317–319.
- 350 Allan, R. P., Soden, B. J., 2008. Atmospheric Warming and the Amplification of Precipitation
351 Extremes. *Science*, 321, 5895, 1481-1484. <https://doi.org/10.1126/science.1160787>
- 352 Blanchet J., Creutin JD., Blanc A. (2021). Retreating winter and strengthening autumn
353 Mediterranean influence on extreme precipitation in the Southwestern Alps over the last
354 60 years. *Environ. Res. Lett.* 16 034056, <https://doi.org/10.1088/1748-9326/abb5cd>

- 355 Borga M., Vezzani C. & Fontana G.D. (2005). Regional Rainfall Depth–Duration–Frequency
 356 Equations for an Alpine Region. *Nat Hazards* 36, 221–235.
 357 <https://doi.org/10.1007/s11069-004-4550-y>
- 358 Chen Y., Paschalis A., Kendon E., Kim D., Onof C. (2021). Changing spatial structure of
 359 summer heavy rainfall, using convection-permitting ensemble. *Geophysical Research*
 360 *Letters*, 48, e2020GL090903. <https://doi.org/10.1029/2020GL090903>
- 361 Chow, V. T., Maidment, D. R., & Mays, L. W. (1988). *Applied hydrology*. McGraw-Hill
- 362 Cristiano, E., ten Veldhuis, M.-C., and van de Giesen, N. (2017). Spatial and temporal variability
 363 of rainfall and their effects on hydrological response in urban areas – a review, *Hydrol.*
 364 *Earth Syst. Sci.*, 21, 3859–3878, <https://doi.org/10.5194/hess-21-3859-2017>
- 365 Fatichi, S., Ivanov, V. Y., Paschalis, A., Peleg, N., Molnar, P., Rimkus, S., et al. (2016).
 366 Uncertainty partition challenges the predictability of vital details of climate change.
 367 *Earth's Future*, 4, 240–251. <https://doi.org/10.1002/2015EF000336>
- 368 Fischer RA, Tippett LHC. (1928). Limiting forms of the frequency distribution of the largest or
 369 smallest member of a sample. *Math Proc Camb Philos Soc* 1928;24(02):180–90.
- 370 Fowler H.J., Lenderink G., Prein, A.F. et al. (2021a) Anthropogenic intensification of short-
 371 duration rainfall extremes. *Nat Rev Earth Environ* 2, 107–122.
 372 <https://doi.org/10.1038/s43017-020-00128-6>
- 373 Fowler H. J., et al. (2021b). Towards advancing scientific knowledge of climate change impacts
 374 on short-duration rainfall extremes. *Phil. Trans. R. Soc. A* 379: 20190542.
 375 <https://doi.org/10.1098/rsta.2019.0542>
- 376 Gilbert, R. O. (1987). *Statistical methods for environmental pollution monitoring*. New York
 377 City: Wiley. <https://doi.org/10.2307/1270090>
- 378 Gnedenko B. (1943). Sur la distribution limite du terme maximum d'une serie aleatoire. *Ann*
 379 *Math* 1943;44(3):423–53.
- 380 Groisman P.Ya., Knight R.W., Easterling D.R., Karl T.R., Hegerl G.C., Razuvaev V.N. (2005).
 381 Trends in intense precipitation in the climate record. (2005) *Journal of Climate*, 18 (9),
 382 pp. 1326-1350. Cited 935 times. doi: 10.1175/JCLI3339.1
- 383 Guerreiro, S.B., Fowler, H.J., Barbero, R. et al. (2018). Detection of continental-scale
 384 intensification of hourly rainfall extremes. *Nature Clim Change* 8, 803–807.
 385 <https://doi.org/10.1038/s41558-018-0245-3>
- 386 Haerter, J. O., P. Berg, and S. Hagemann (2010), Heavy rain intensity distributions on varying
 387 time scales and at different temperatures, *J. Geophys. Res.*, 115, D17102,
 388 doi:10.1029/2009JD013384
- 389 Helsel, D. R., & Frans, L. M. (2006). Regional Kendall test for trend. *Environmental Science &*
 390 *Technology*, 40(13), 4066–4073.
- 391 Hirsch, R. M.; Slack, J. R. (1984). A nonparametric trend test for seasonal data with serial
 392 dependence. *Water Resour. Res.* 1984, 20, 727-732
- 393 Iliopoulou T, Koutsoyiannis D. (2020). Projecting the future of rainfall extremes: Better classic
 394 than trendy. *J. Hydrol.*, 588 , p. 125005, <https://doi.org/10.1016/j.jhydrol.2020.125005>.

- 395 Kendall, M. G. (1975). Rank Correlation Methods. New York, NY: Oxford University Press.
- 396 Lenderink, G., and E. van Meijgaard (2008), Increase in hourly precipitation extremes beyond
397 expectations from temperature changes, *Nat. Geosci.*, 1, 511–514.
- 398 Libertino A., Ganora D., & Claps P. (2019). Evidence for increasing rainfall extremes remains
399 elusive at large spatial scales: The case of Italy. *Geophysical Research Letters*, 46, 7437–
400 7446. <https://doi.org/10.1029/2019GL083371>
- 401 Mann, H. B. (1954) Non-parametric tests against trend. *Econometrica* 1945, 13, 245-259.
- 402 Marani M., Ignaccolo M. (2015). A metastatistical approach to rainfall extremes, *Advances in*
403 *Water Resources*, Volume 79, 2015, Pages 121-126, ISSN 0309-1708,
404 <https://doi.org/10.1016/j.advwatres.2015.03.001>.
- 405 Marchi L., Borga M., Preciso E., Gaume E. (2010). Characterisation of selected extreme flash
406 floods in Europe and implications for flood risk management. *J. Hydrol.*, 394, pp. 118-
407 133, <https://doi.org/10.1016/j.jhydrol.2010.07.017>
- 408 Markonis, Y., Papalexiou, S. M., Martinkova, M., & Hanel, M. (2019). Assessment of water cycle
409 intensification over land using a multi source global gridded precipitation dataset. *Journal*
410 *of Geophysical Research: Atmospheres*, <https://doi.org/10.1029/2019JD030855>
- 411 Marra, F., Armon, M., Adam, O., Zocatelli, D., Gazal, O., Garfinkel, C. I., et al. (2021).
412 Towards narrowing uncertainty in future projections of local extreme precipitation.
413 *Geophysical Research Letters*, 48, e2020GL091823.
414 <https://doi.org/10.1029/2020GL091823>
- 415 Marra, F., Nikolopoulos, E. I., Anagnostou, E. N., & Morin, E. (2018). Metastatistical extreme
416 value analysis of hourly rainfall from short records: Estimation of high quantiles and
417 impact of measurement errors. *Advances in Water Resources*, 117, 27–39.
418 <https://doi.org/10.1016/j.advwatres.2018.05.001>
- 419 Marra, F., Zocatelli, D., Armon, M., & Morin, E. (2019). A simplified MEV formulation to
420 model extremes emerging from multiple nonstationary underlying processes. *Advances in*
421 *Water Resources*, 127, 280–290. <https://doi.org/10.1016/j.advwatres.2019.04.002>
- 422 Marra, F., Borga, M., & Morin, E. (2020). A unified framework for extreme subdaily
423 precipitation frequency analyses based on ordinary events. *Geophysical Research Letters*,
424 47, e2020GL090209.
- 425 Min SK, Zhang X, Zwiers F, Friederichs P, Hense A (2009) Signal detectability in extreme
426 precipitation changes assessed from twentieth century climate simulations. *Clim Dyn*
427 32:95–111
- 428 Miniussi, A., & Marani, M. (2020). Estimation of daily rainfall extremes through the
429 metastatistical extreme value distribution: Uncertainty minimization and implications for
430 trend detection. *Water Resources Research*, 56, e2019WR026535.
431 <https://doi.org/10.1029/2019WR026535>
- 432 Miniussi, A., Villarini, G., & Marani, M. (2020). Analyses through the metastatistical extreme
433 value distribution identify contributions of tropical cyclones to rainfall extremes in the
434 eastern United States. *Geophysical Research Letters*, 47, e2020GL087238.
435 <https://doi.org/10.1029/2020GL087238>

- 436 Moustakis, Y., Papalexiou, S. M., Onof, C. J., & Paschalis, A. (2021). Seasonality, intensity, and
 437 duration of rainfall extremes change in a warmer climate. *Earth's Future*, 9,
 438 e2020EF001824. <https://doi.org/10.1029/2020EF001824>
- 439 Myhre, G., Alterskjær, K., Stjern, C.W. et al. Frequency of extreme precipitation increases
 440 extensively with event rareness under global warming. *Sci Rep* 9, 16063 (2019).
 441 <https://doi.org/10.1038/s41598-019-52277-4>
- 442 Papalexiou, S. M., AghaKouchak, A., & Foufoula-Georgiou, E. (2018). A diagnostic framework
 443 for understanding climatology of tails of hourly precipitation extremes in the United
 444 States. *Water Resources Research*, 54(9), 6725–6738.
 445 <https://doi.org/10.1029/2018WR022732>
- 446 Papalexiou, S. M., & Montanari, A. (2019). Global and regional increase of precipitation
 447 extremes under global warming. *Water Resources Research*, 55,4901–4914.
 448 <https://doi.org/10.1029/2018WR024067>
- 449 Paprotny, D., Sebastian, A., Morales-Napoles, O., & Jonkman, S. N. (2018). Trends in flood
 450 losses in Europe over the past 150 years. *Nature Communications*, 9, 1985
- 451 Pendergrass, A. G. (2018). What precipitation is extreme? *Science*, 360, 6393.
 452 <https://doi.org/10.1126/science.aat1871>
- 453 Pendergrass, A.G. (2020). Changing Degree of Convective Organization as a Mechanism for
 454 Dynamic Changes in Extreme Precipitation. *Curr Clim Change Rep* 6, 47–54.
 455 <https://doi.org/10.1007/s40641-020-00157-9>
- 456 Pendergrass, A. G., Hartman, D. L. (2014). The Atmospheric Energy Constraint on Global-Mean
 457 Precipitation Change. *J. Climate*, 27, 2, 757-768, <https://doi.org/10.1175/JCLI-D-13-00163.1>
- 459 Prosdocimi, I., Kjeldsen, T. Parametrisation of change-permitting extreme value models and its
 460 impact on the description of change. *Stoch Environ Res Risk Assess* 35, 307–324 (2021).
 461 <https://doi.org/10.1007/s00477-020-01940-8>
- 462 Schär C., N. Ban, E.M. Fischer, et al., 2016. Percentile indices for assessing changes in heavy
 463 precipitation events. *Clim. Change*, 137, 201-216, <https://doi.org/10.1007/s10584-016-1669-2>
- 465 Sen PK (1968). Estimates of the regression coefficient based on Kendall's tau, *J. Am. Statist.*
 466 *Assoc.*, 63, 1379–1389, <http://doi.org/10.1080/01621459.1968.10480934>
- 467 Serinaldi, F., & Kilsby, C. G. (2015). Stationarity is undead: Uncertainty dominates the
 468 distribution of extremes. *Advances in Water Resources*, 77, 17–36.
- 469 Trenberth, K. E., A. Dai, R. M. Rasmussen, and D. B. Parsons (2003), The changing character of
 470 precipitation, *Bull. Am. Meteorol. Soc.*, 84, 1205– 1217.
- 471 van Belle G., Hughes, J. P. (1984) Nonparametric tests for trend in water quality. *Water Resour.*
 472 *Res.* 1984, 20, 127-136.
- 473 Zheng F., Westra S., Leonard M. (2015). Opposing local precipitation extremes. *Nature Clim*
 474 *Change* 5, 389–390. <https://doi.org/10.1038/nclimate2579>

475 Zorzetto E., Botter G., Marani M. (2016). On the emergence of rainfall extremes from ordinary
476 events. *Geophysical Research Letters*, 43, 8076–8082.
477 <https://doi.org/10.1002/2016GL069445>